Multiple observation processes in spatial capture–recapture models: How much do we gain?

Mahdieh Tourani,[1,4] Pierre Dupont,[1] Muhammad Ali Nawaz,[2,3] and Richard Bischof[1]

[1]*Faculty of Environmental Sciences and Natural Resource Management, Norwegian University of Life Sciences, P.O. Box 5003,1432Ås, Norway*
[2]*Department of Animal Sciences, Quaid-i-Azam University, Islamabad 44000 Pakistan*
[3]*Snow Leopard Trust, Islamabad 44000 Pakistan*

Abstract. Population monitoring data may originate from multiple methods and are often sparse and fraught with incomplete information due to practical and economic constraints. Models that can integrate multiple survey methods and are able to cope with incomplete data may help investigators exploit available information more thoroughly. Here, we developed an integrated spatial capture–recapture (SCR) model to incorporate multiple data sources with imperfect individual identification. We contrast inferences drawn from this model with alternate models incorporating only subsets of the data available. Using extensive simulations and an empirical example of multi-method brown bear (*Ursus arctos*) monitoring data from northern Pakistan, we quantified the benefits of including multiple sources of information in SCR models in terms of parameter precision and bias. Our multiple observation processes SCR model (MOP) yielded a more complete picture of the underlying processes, reduced bias, and led to more precise parameter estimates. Our results suggest that the greatest gains from integrated SCR models can be expected in situations where detection probability is low, a large proportion of detections is not attributable to individuals, and the degree of overlap between individual home ranges is low.

Key words: camera trap; data integration; large carnivore; multiple observation process; noninvasive monitoring; simulation; spatial capture–recapture.

Introduction

Wildlife monitoring is an integral part of applied ecology, providing valuable information about populations in order to assess their status and inform recovery or control. One of the primary challenges in wildlife monitoring arises from the failure to detect all individuals in a population. For decades, capture–recapture (CR) methods were used to deal with this challenge by estimating detection probability and accounting for it during the estimation of ecological parameters such as abundance and vital rates (Lukacs and Burnham 2005). A comparatively recent development, spatial capture–recapture (SCR; Efford 2004, Royle et al. 2018) additionally uses the information in the spatial configuration of individual detections to directly estimate density when data are available only for a subset of the population.

Sparse data sets are common in SCR studies, because this framework is particularly popular for inventory and monitoring of rare or elusive species, to estimate density with data obtained noninvasively over large areas (e.g., Sollmann et al. 2013b). This poses a challenge, because SCR models, like non-spatial CR models (Gerber et al. 2014), are known to return biased and imprecise estimates when fit to sparse data (Marques et al. 2011, Sollmann et al. 2012). Moreover, noninvasive monitoring methods often yield detections that are not attributable to specific individuals (e.g., incomplete genotype information in genetic capture–recapture studies or camera trap data with inconclusive individual designation). Discarding these unidentified detections further reduces the amount of data used for estimation (Augustine et al. 2019).

Nowadays, many species inventories combine multiple survey methods, such as noninvasive DNA sampling,

Statistical Reports

camera trapping, sign surveys, or physical mark–recapture to maximize the amount of data (Blanc et al. 2014, Clare et al. 2017, Burgar et al. 2018, Murphy et al. 2018). One way to better exploit the available information is integrated modeling, the joint analysis of multiple data sets traditionally analyzed separately (Besbeas et al. 2002). This trend has also found its way into the SCR framework (Gopalaswamy et al. 2012, Sollmann et al. 2013b). The idea of integrated modeling is to combine into one analysis different data sets that contain (potentially partial) information about the same underlying ecological processes of interest. The different data sets do not necessarily originate from different survey methods (e.g., individual detections from DNA-sampling and camera trapping; Sollmann et al. 2013b) but they can also represent different data types collected using the same survey method. For example, this is the case of spatial mark–resight models (SMR) that combine detections of the marked, identified, and unmarked, always unidentified, parts of a population collected using camera traps (Rich et al. 2014). Traditionally, unidentified detections are discarded further reducing available data for analysis. Recently, generalized SMR proposed to deal with this situation (Whittington et al. 2018). However, these models still rely on the assumption that marked individuals are always recognized as marked if detected (Royle et al. 2013). This assumption is violated when the marking status is not observable with certainty. For example, in case of tag loss an individual may be misclassified as unmarked when it belongs to the marked part of the population. Poor quality pictures in camera trapping are another example for uncertain mark status for a detection usually leading to that detection being discarded.

Here we describe an integrated SCR model that combines data sets originating from different survey types, each with potentially varying degree of completeness in terms of the proportion of individually identified detections. In addition, this model relaxes the assumption that marked individuals are always recognized as marked. We then ask to what extent the integrated analysis of multiple sources of information boosts our ability to draw inferences from monitoring data by comparing the precision and bias of parameter estimates from four models using different subsets of the available data.

Model 1: classic SCR, uses only identified detections from a single survey method.
Model 2: integrates identified and unidentified detections from a single survey method.
Model 3: integrates identified detections from one survey method and unidentified detections from a second independent survey method.
Model 4: the multiple observation processes (MOP) SCR model that combines all data sets.

Finally, we showcase our modeling approach by applying it to a sparse multi-method survey data set on brown bear (*Ursus arctos*) from the western Himalayas in Pakistan.

METHODS

Model specification

We developed an integrated Bayesian SCR model composed of two hierarchical levels. The first one describes the underlying ecological process of interest (i.e., density) and the second one describes the associated observation processes (Fig. 1).

Ecological process.— The ecological process describes population density, which arises from the distribution of individuals in space. Following a homogeneous point process (Royle et al. 2018), the positions of individual activity centers s_i are uniformly distributed across the habitat S, the spatial extent within which individual activity centers can be placed:

$$s_i \sim \text{Uniform}(S) \tag{1}$$

To account for the fact that some individuals in the population may never be detected, we used a data-augmentation approach (Royle et al. 2007). For all M individuals (M much larger than the unknown true population size), we modeled inclusion in the population through a latent state variable z_i, governed by the inclusion probability Ψ:

$$z_i \sim \text{Bernoulli}(\Psi) \tag{2}$$

Population size N is then the sum of individuals included in the population:

$$N = \sum_{i=1}^{M} z_i \tag{3}$$

Observation processes.— In SCR, the classic observation model describes the probability of detecting individual i at discrete locations (i.e., detectors) conditional on its s_i location. In our integrated model, we considered K different survey types deployed simultaneously corresponding to K independent sets of detectors, each composed of J^k detectors. Considering the commonly used half-normal detection function (Borchers and Efford 2008), we expressed probability p_{ij}^k of detecting individual i at the jth detector of the detector set k as:

$$p_{ij}^k = p_0^k \times e^{-\frac{\left(d_{ij}^k\right)^2}{2\sigma^2}} \times z_i, \tag{4}$$

where d_{ij}^k is the distance between the individual's activity center s_i and detector j^k; p_0^k is the magnitude parameter for survey type k; and σ is the scale parameter. While
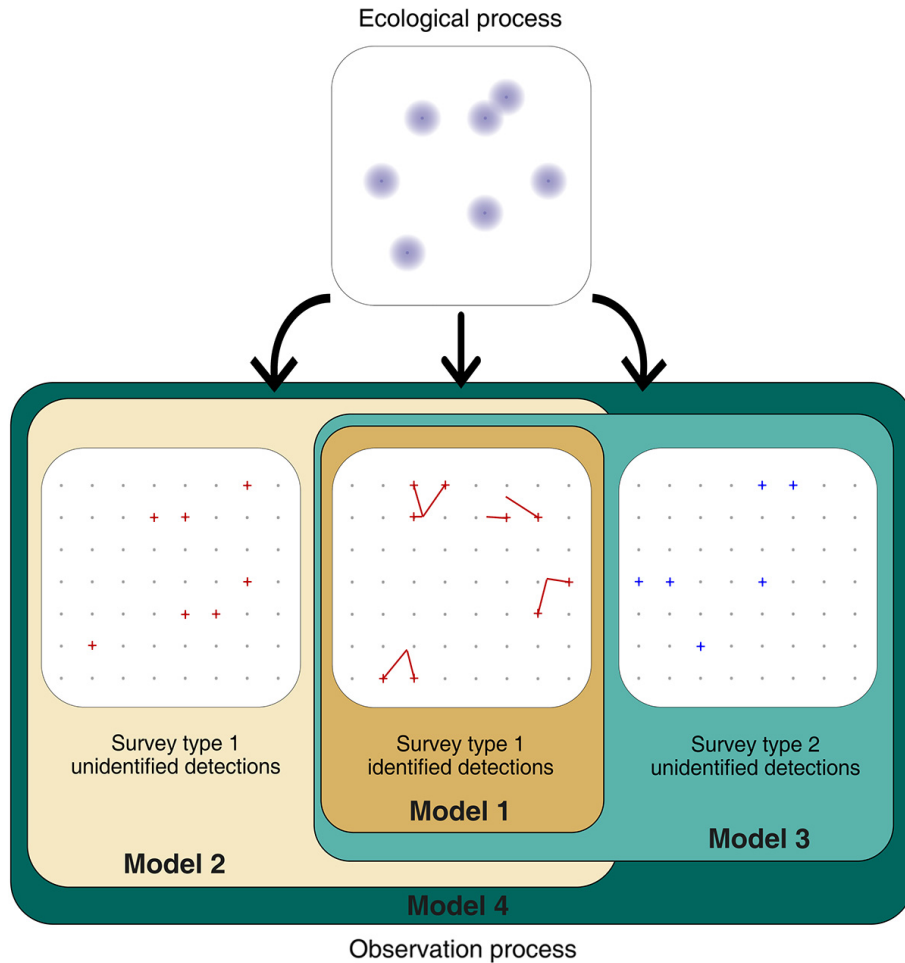
Ecological process

Fig. 1. Hierarchical structure of the four spatial capture–recapture (SCR) models integrating different combinations of data. The top box shows the distribution of latent individual activity centers, with associated detection probability indicated as gradual shading. Lower boxes show detections of those individuals at detectors (gray points). Survey type 1 yields detections both with (red plus signs, left panel) and without individual identity (lines connecting detections to individual activity centers, middle panel). Survey type 2 yields detections without individual identity indicated by blue crosses.

the baseline detection probability is specific to each survey type, the scale parameter is shared as we assume it arises from the ecological process (e.g., space use). Alternatively, σ could be survey type-specific if it is linked with the detection process rather than animal space use (e.g., acoustic methods; Efford et al. 2009), as long as each survey type contributes detections of identified individuals at multiple detectors.

In many situations, detections cannot be linked to an individual with certainty, yet the spatial information of unidentified detections can be used in an integrated SCR framework by modeling the probability of obtaining unidentified detections conditional on the latent activity centers of individuals in the population. Individual detections might not be independent (e.g., temporal correlation of fecal samples), which results in violation of Poisson assumptions (Royle et al. 2013). This is the case of our bear study where the sampling process did not allow us to consider the number of detections as real

counts. We therefore considered binary detector-level detections, instead of counts of unidentified detections, and expressed the probability to collect at least one unidentified detection at detector j from survey type k as:

$$\dot{p}_J^k = 1 - \prod_{i=1}^{M} \left(1 - p_{ij}^k \times \left(1 - \alpha^k\right)\right), \qquad (5)$$

where α^k is the probability that any sample from survey type k be identified. Following this formulation, the K matrices of individually identified detections y_{ij}^k for the M individuals at J^k detectors are the outcome of a Bernoulli process with probability of detection p_{ij}^k:

$$y_{ij}^k \sim \text{Bernoulli}\left(p_{ij}^k \cdot \alpha^k\right) \qquad (6)$$

Detections without individual ID are compiled as K vectors of zeros and ones of length J^k, where $\dot{y}_j^k$

represents the presence/absence of at least one unidentified detection at detector j^k:

$$\dot{y}_J^k \sim \text{Bernoulli}\big(\dot{p}_J^k\big) \qquad (7)$$

Under this formulation, identified and unidentified components of a given survey type k share parameters p_0^k and α^k, while σ and N (or density; z_i: individual inclusion) are shared by all observation processes. When all observation models are combined in a joint likelihood in the MOP model, both identified and unidentified detections from multiple survey types inform about the same ecological parameters (σ and N), thus potentially improving inferences.

Simulation study

We used simulations to quantify and compare the performance of models with different levels of data integration. Specifically, we were interested in the consequences of data integration on the precision and bias of two key parameters, N and σ, under different scenarios of population size, individual home range overlap, proportion of identified detections, and overall detectability.

Although SCR studies often use multiple occasions, this is not necessary (Efford et al. 2009) and we simulated a population surveyed with $k = 2$ survey types during a single occasion. Method 1 yields both identified and unidentified detections with variable levels of identification ($\alpha = 0.25, 0.50,$ and 0.75). This is, for example, the case in most DNA-based studies where some DNA samples fail to produce definite identification. We considered that method 2 could only generate unidentified detections ($\alpha = 0$), as would be the case in a camera-trap study of a species without unique external markings. In a square habitat of 50×50 arbitrary distance units without a surrounding unsampled buffer area, we randomly drew either 30 or 50 individuals' s_i positions, following Eq. 1. Although many SCR studies incorporate an unsampled buffer into their state space, not doing so allowed us to use the same state-space for all scenarios, instead of dealing with variable buffer sizes for each σ scenario, which would have made comparisons between simulations difficult (forcing either variable densities or variable population sizes). We defined two independent detector grids, placed 1.0 and 1.2 distance units apart, leading to $J^1 = 2,500$ and $J^2 = 1,764$ detectors, respectively. We then simulated individual detections for three levels of σ (1, 2, or 3 distance units) to generate increasing levels of overlap between individual home ranges (Efford and Hunter 2018). To avoid any confounding effect of higher detectability associated with higher σ, we parameterized our simulations using a constant effective sampling area A_0 (Borchers and Efford 2008). This allowed us to calculate a different value of p_0 for each σ while keeping the overall individual detectability constant

$$p_0 = 1 - \exp-\big(A_0/2\pi\sigma^2\big) \qquad (8)$$

Detection parameters were chosen so that approximately 65% or 85% of the population was detected by the two survey types combined, corresponding to levels of detections of approximately 50% or 70% detected by survey method 1, and 30% or 50% by method 2, respectively. We generated individual detection histories y_{ij}^1 and y_{ij}^2 (Eq. 6), using the detection probabilities defined in Eq. 4. As survey type 1 yields both identified and unidentified detections, we randomly retained individual detection histories with three levels of identification probability ($\alpha = 0.25, 0.50,$ and 0.75). For example, considering high detections, if 85% of the population was detected, given the identification probability of 0.75, we only detected and identified 64% of the population in the best-case scenario, and only 21% in the worst-case scenario (low detection: 65%, $\alpha = 0.25$). We then created the unidentified data set $\dot{y}_J^1$ by aggregating unidentified detections into one vector of length J^1 composed of one when at least one detection was collected, and zero if no detection occurred at detector j.

We generated 50 data sets for each set of parameters before fitting all four models (Appendix S1) to each. We fitted all models to the simulated data using NIMBLE (version 0.6-9, de Valpine et al. 2017) and R (version 3.5.2, R Development Core Team 2018). We drew from three chains, 15,000 MCMC samples each, and the initial 5,000 samples were discarded as burn-in. We assessed convergence using the potential scale reduction value for all parameters and by inspecting the mixing of the chains using trace-plots (Brooks and Gelman 1998). We performed a frequentist validation of our Bayesian model and evaluated its performance by checking the relative bias (RB) of the mode of the posterior distribution, the coefficient of variation (CV) and the coverage of the 95% credible intervals of N and σ (Walter and Moore 2005).

Himalayan brown bear in northern Pakistan

The development of the MOP SCR model was originally motivated by our intent to estimate abundance of Himalayan brown bears in northern Pakistan's Deosai National Park. The bear population of Deosai was monitored across an area of 2,262 km^2 through both noninvasive DNA-sampling (survey type 1; consisting of both identified and unidentified observations) and camera trapping (survey type 2; only unidentified observations) from 23 September to 9 November 2012. This data set is a good example of the different challenges faced by surveys of rare and elusive species, due to remoteness, high elevation, and imposing logistic challenges. To highlight the benefits of data integration for a case study, we fitted the same four models to the bear data and compared estimates of parameters N and σ (see Appendix S2 for a detailed description of the data collection and analysis).

Results

Simulations

Of the 7,200 simulation runs, 6,478 converged: 1,487 for model 1, 1,561 model 2, 1,686 model 3 and 1,744 model 4. We considered only these runs in all further analyses (Appendix S3: Table S1). Coverage for both N and σ was nominal in all models (Appendix S3: Table S2). In all simulation scenarios, data integration led to conspicuous improvements in precision and reduced bias in estimates of parameters N and σ (Fig. 2). Gains in precision from data integration increased with decreasing overall detection probability, decreasing proportion of identified detections, and decreasing overlap between individual home ranges. In the situation where data were the most sparse (and gains greatest), i.e., when detectability, identification probability and overlap were low ($\alpha = 0.25$ and $\sigma = 1$), we obtained an 80% CV reduction for N with model 4 (CV $(N) = 0.25$), compared to model 1 (CV$(N) = 1.2$). By comparison, the reduction in CV was only 20% (CV $(N)_{\text{Model 4}} = 0.24$ and CV$(N)_{\text{Model 1}} = 0.29$), when detection was high, $\alpha = 0.75$, and $\sigma = 3$. The pattern was similar for σ with up to a 90% CV reduction (CV $(\sigma)_{\text{Model 4}} = 0.2$ and CV$(\sigma)_{\text{Model 1}} = 1.6$) at low detectability, identification probability and overlap to only 30% (CV$(\sigma)_{\text{Model 4}} = 0.16$ and CV$(\sigma)_{\text{Model 1}} = 0.24$) at high detectability, identification probability and overlap.

Similarly, data integration led to a reduction in bias in all scenarios. This effect was greater with decreasing overall detectability, decreasing identification probability, and decreasing overlap between individual home ranges (Fig. 2). For example, the mean relative bias in N obtained with model 4 was 90% smaller (RB$(N)_{\text{Model 4}} = -0.03$) than that of model 1 (RB$(N)_{\text{Model 1}} = -0.4$) when detectability was low, $\alpha = 0.25$, and $\sigma = 1$. By comparison, when detectability was high, $\alpha = 0.75$, and $\sigma = 3$, the reduction in RB was only 20% (RB$(N)_{\text{Model 4}} = -0.04$ and RB$(N)_{\text{Model 1}} = -0.05$). Again, the pattern was similar for σ: 80% reduction in RB (RB$(\sigma)_{\text{Model 4}} = -0.09$ and RB $(\sigma)_{\text{Model 1}} = -0.6$) versus 20% (RB$(\sigma)_{\text{Model 4}} = -0.07$ and RB$(\sigma)_{\text{Model 1}} = -0.09$) at low and high detectability, identification probability and overlap, respectively.

Empirical example: Himalayan brown bear in northern Pakistan

The identified part of the data contained 22 DNA samples from 14 individual bears collected at 19 different locations. Of these, only four individuals were detected more than once (one detected four times; two detected three times, and one detected two times). Our data set included an additional 21 bear DNA samples lacking individual identification. The camera trap data contributed an additional eight camera trap locations where bears were detected at least once. Using the MOP model (model 4), we estimated the mode of brown bear density at 22 bear/1,000 km^2 (95% CI = 14–30) and the spatial scale parameter σ at 3.2 km (95% CI = 2.1–5). The point estimates produced by the four models were similar (Fig. 3, Table S2). However, data integration in the model 4 led to pronounced improvements in the precision of bear population size (up to 30% reduction in standard deviation [SD]) and space-use parameter estimates (up to 40% reduction in SD), compared to model 1 (Appendix S2).

Discussion

In both simulations and empirical analyses, data integration led to more reliable estimates, i.e., increased precision and reduced bias. We used a frequentist validation of our Bayesian modeling approach, and our simulation study confirmed that the MOP model reliably and precisely estimated density and space-use when using additional information from unidentified observations and multiple survey types. This has direct implications for inferences in real-life, where the integration of auxiliary data, if available, can mitigate the problems associated with data sparsity. We were also able to identify under which conditions the benefits of integration were most substantial.

1.. Low detectability; the lower the proportion of individuals detected, the higher the relative importance of any additional information. When very few individuals are detected, even a single unidentified detection far away from all other detections contains valuable information as it most likely originated from a previously undetected individual.
2.. Minimal home range overlap; the certainty with which the integrated model associates an unidentified detection to a given individual (and therefore the precision of N) increases as the overlap between individual home ranges decreases (Efford and Hunter 2018). When individual detections are well segregated, an unidentified sample will be assigned with a high level of certainty to the closest individual, or, if no individuals were detected in proximity, to a new individual. This should prove particularly useful for territorial species or low-density populations where individual detections minimally overlap, i.e., many of the species commonly studied using SCR models (e.g., Gopalaswamy et al. 2012, Sollmann et al. 2013b).
3.. High proportion of unidentified detections; SCR models that ignore unidentified detections risk ignoring a substantial source of information. Although less informative, unidentified detections can still inform about the spatial configuration of individuals, i.e., density, thus reducing the bias and uncertainty around both the scale parameter and population size. This is particularly pronounced under simulated scenarios where only a small percentage of the detections can be assigned to individuals. Conversely, when overall detection and
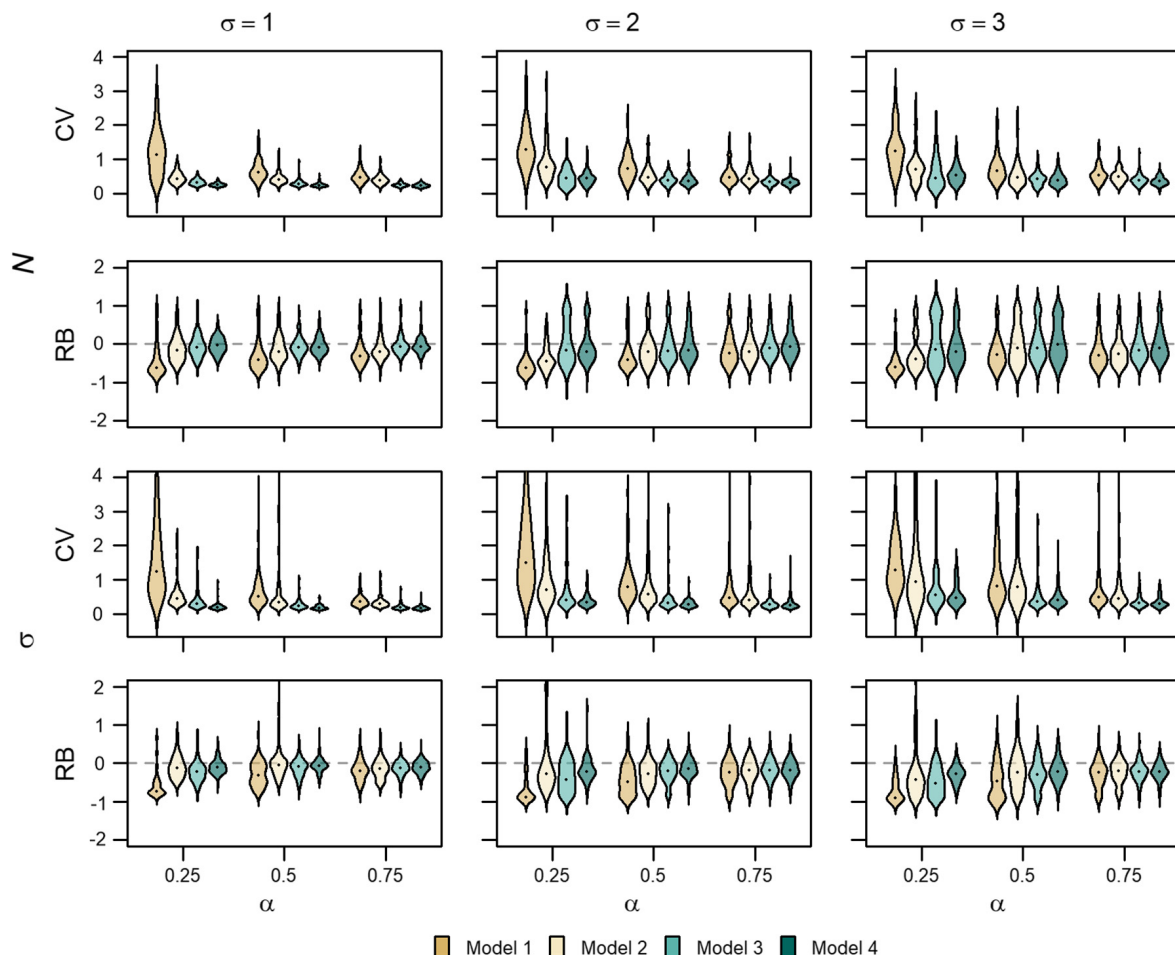
Statistical Reports

Statistical Reports

Fig. 2. Violin plots show coefficient of variation (CV) and relative bias (RB) of population size (*N*) and spatial scale parameter of the detection function (σ), under the low detectability scenario for different levels of home-ranges overlap (higher σ = higher overlap) and identification (α). Points indicate medians.

identification is high, the gains from integration of additional data from unidentified detections are minimal. In such cases, the benefits of data integration are likely outweighed by its cost, namely increased model complexity and computation time.

Despite employing both camera trapping and noninvasive DNA sampling, monitoring data of brown bears in our study area remained sparse. Furthermore, only 50% of DNA samples were attributable to individuals and none of the camera trap photos. Integration (including DNA samples without individual identity and camera trap photos), led to improvements in the precision of bear population size and space-use parameter estimates, compared to solely using identified DNA samples. Furthermore, data integration increased the spatial coverage of detectors and detections, which boosted the spatial detail and extent of the model-derived realized density surface (Appendix S2: Fig. S1).

The MOP model is an SCR model that integrates any number of additional survey methods that produce spatially explicit observation data, regardless of whether these methods yield individually identifiable observations or not. Unmarked SCR models that use only unidentified detections are known to have identifiability issues unless an informative prior is used (e.g., Chandler and Royle 2013, Ramsey et al. 2015) or additional data contribute information about individual space-use (e.g., telemetry data in Sollmann et al. 2013*a*). Informative priors can also be used in the MOP model, but even without them, the space-use parameter becomes directly estimable by integrating a proportion of data with identified detections. The MOP model can also allocate undesignated detections to marked or unmarked individuals. This is particularly important when survey method yields observations within which mark status is independent of identification status (e.g., noninvasive DNA sampling).

The observation model of the MOP could also be reformulated as a Poisson counting process (Borchers and Fewster 2016). In this situation, estimates are likely to be even more precise due to increased information in count
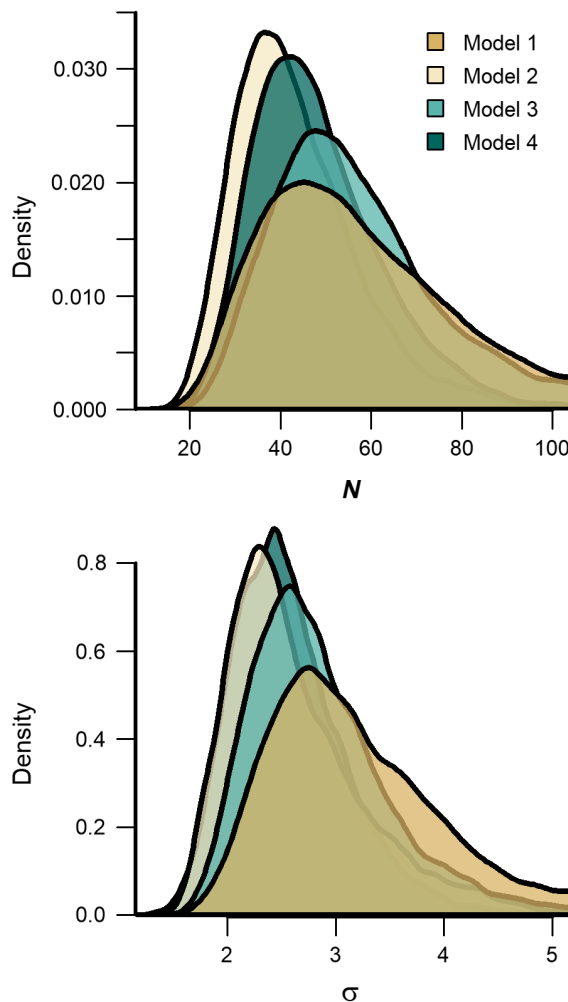
FIG. 3. Posterior densities of the population size (*N*) and spatial scale (σ) estimates from the four models for the brown bear population in Deosai National Park, Pakistan (see also Fig. 1).

In cases of survey type-specific σ, the link between detection processes is broken and the CR data can only be integrated with unidentified detections as in integration of CR and occupancy (Blanc et al. 2014).

Although it is often assumed that reducing sample size will lead to decreased precision without introducing bias, this is clearly not the case when using sparse data, as we have shown here, where negative bias in parameter estimates was typical when true population size was small. By discarding detections with uncertain individual identity, investigators may inadvertently risk obtaining biased estimates. In addition, our observation of negative bias in estimates of *N* in all models when the σ estimate was biased upwards should be investigated rigorously. This pattern could be associated with identifiability issues (Lele et al. 2010, Ponciano et al. 2012) and further research on this topic for SCR models is greatly needed.

The MOP model can also be adjusted to accommodate other extensions of the SCR framework, such as covariates on focal parameters (Borchers and Fewster 2016), non-Euclidean distances (Royle et al. 2018), or it can be re-formulated as an open population SCR model to incorporate population dynamics (Bischof et al. 2016). Finally, we emphasize that, while the incorporation of multiple observation processes can help mitigate the challenges brought on by data sparsity, this does not diminish the necessity for appropriate survey design, lest investigators are to draw erroneous inferences.

data compared to binary data. Here, we used a Bernoulli observation model because the data collection procedure did not allow us to consider multiple samples collected at the same location as independent. This is also true of many studies that use hair-snares to collect DNA samples without a way to designate samples to separate visits of an individual at a given detector. Each observation process in our model can be re-formulated to include partial/uncertain identification (Augustine et al. 2019) upon availability of such data.

Of the models tested here, the MOP model makes the best use of noninvasive monitoring data. By informing model parameters that are shared between observation processes, it may help fitting SCR models that otherwise would have failed to converge and return reliable estimates. The assumption of a shared σ between detection processes always holds for identified and unidentified detections coming from the same data collection scheme.

LITERATURE CITED

Augustine, B. C., J. A. Royle, S. M. Murphy, R. B. Chandler, J. J. Cox, and M. J. Kelly. 2019. Spatial capture–recapture for categorically marked populations with an application to genetic capture–recapture. Ecosphere 10:e02627.

Besbeas, P., S. N. Freeman, B. J. T. Morgan, and E. A. Catchpole. 2002. Integrating mark-recapture-recovery and census data to estimate animal abundance and demographic parameters. Biometrics 58:540–547.

Bischof, R., H. Brøseth, and O. Gimenez. 2016. Wildlife in a politically divided world: Insularism inflates estimates of brown bear abundance. Conservation Letters 9:122–130.

Blanc, L., E. Marboutin, S. Gatti, F. Zimmermann, O. Gimenez, and H. McCallum. 2014. Improving abundance estimation by combining capture-recapture and occupancy data: example with a large carnivore. Journal of Applied Ecology 51:1733–1739.

Borchers, D. L., and M. G. Efford. 2008. Spatially explicit maximum likelihood methods for capture-recapture studies. Biometrics 64:377–385.

Borchers, D. L., and R. M. Fewster. 2016. Spatial capture–recapture models. Statistical Science 31:219–232.

Brooks, S. P., and A. Gelman. 1998. General methods for monitoring convergence of iterative simulations. Journal of Computational and Graphical Statistics 7:434–455.

Burgar, J. M., F. E. C. Stewart, J. P. Volpe, J. T. Fisher, and A. C. Burton. 2018. Estimating density for species conservation: Comparing camera trap spatial count models to genetic spatial capture-recapture models. Global Ecology and Conservation 15:e00411.

Chandler, R. B., and J. A. Royle. 2013. Spatially explicit models for inference about density in unmarked or partially marked populations. Annals of Applied Statistics 7:936–954.

Clare, J., S. T. Mckinney, J. E. Depue, and C. S. Loftin. 2017. Pairing field methods to improve inference in wildlife surveys. Ecological Applications 27:2031–2047.

de Valpine, P., D. Turek, C. J. Paciorek, C. Anderson-Bergman, D. T. Lang, and R. Bodik. 2017. Programming with models: writing statistical algorithms for general model structures with NIMBLE. Journal of Computational and Graphical Statistics 26:403–413.

Efford, M. G. 2004. Density estimation in live-trapping studies. Oikos 106:598–610.

Efford, M. G., D. K. Dawson, and D. L. Borchers. 2009. Population density estimated from locations of individuals on a passive detector array. Ecology 90:2676–2682.

Efford, M. G., and C. M. Hunter. 2018. Spatial capture-mark-resight estimation of animal population density. Biometrics 74:411–420.

Gerber, B. D., J. S. Ivan, and K. P. Burnham. 2014. Estimating the abundance of rare and elusive carnivores from photographic-sampling data when the population size is very small. Population Ecology 56:463–470.

Gopalaswamy, A. M., J. A. Royle, M. Delampady, J. D. Nichols, K. U. Karanth, and D. W. W. Macdonald. 2012. Density estimation in tiger populations: combining information for strong inference. Ecology 93:1741–1751.

Lele, S., R. K. Nadeem, and B. Schmuland. 2010. Estimability and likelihood inference for generalized linear mixed models using data cloning. Journal of the American Statistical Association 105:1617–1625.

Lukacs, P. M., and K. P. Burnham. 2005. Review of capture-recapture methods applicable to noninvasive genetic sampling: review of DNA-based capture-recapture. Molecular Ecology 14:3909–3919.

Marques, T. A., L. Thomas, and J. A. Royle. 2011. A hierarchical model for spatial capture-recapture data: comment. Ecology 92:526–528.

Murphy, S., B. Augustine, J. R. Adams, L. P. Waits, and J. J. Cox. 2018. Integrating multiple genetic detection methods to estimate population density of social and territorial carnivores. Ecosphere 9:e02479.

Ponciano, J. M., J. G. Burleigh, E. L. Braun, and M. L. Taper. 2012. Assessing parameter identifiability in phylogenetic models using data cloning. Systematic Biology 61:955–972.

R Development Core Team. 2018. R: a language and environment for statistical computing. R Foundation for Statistical Computing, Vienna, Austria. https://www.R-project.org/

Ramsey, D. S. L., P. A. Caley, and A. Robley. 2015. Estimating population density from presence-absence data using a spatially explicit model. Journal of Wildlife Management 79:491–499.

Rich, L., M. J. Kelly, R. Sollmann, A. J. Noss, L. Maffei, R. L. Arispe, A. Paviolo, C. D. De Angelo, Y. E. Di Blanco, and M. S. Di Bitetti. 2014. Comparing capture-recapture, mark-resight, and spatial mark-resight models for estimating puma densities via camera traps. Journal of Mammalogy 95:382–391.

Royle, J. A., R. B. Chandler, R. Sollmann, and B. Gardner. 2013. Spatial capture-recapture. Academic Press, Cambridge, Massachusetts, USA.

Royle, J. A., R. M. Dorazio, and W. A. Link. 2007. Analysis of multinomial models with unknown index using data augmentation. Journal of Computational and Graphical Statistics 16:67–85.

Royle, J. A., A. K. Fuller, and C. Sutherland. 2018. Unifying population and landscape ecology with spatial capture-recapture. Ecography 41:444–456.

Sollmann, R., B. Gardner, and J. L. Belant. 2012. How does spatial study design influence density estimates from spatial capture-recapture models? PLoS ONE 7:e34575.

Sollmann, R., B. Gardner, A. W. Parsons, J. J. Stocking, B. T. McClintock, T. R. Simons, K. H. Pollock, and A. F. O'Connell. 2013a. A spatial mark–resight model augmented with telemetry data. Ecology 94:553–559.

Sollmann, R., N. M. Tôrres, M. M. Furtado, A. T. de Almeida Jácomo, F. Palomares, S. Roques, and L. Silveira. 2013b. Combining camera-trapping and noninvasive genetic data in a spatial capture–recapture framework improves density estimates for the jaguar. Biological Conservation 167:242–247.

Walter, B. A., and J. L. Moore. 2005. The concepts of bias, precision and accuracy, and their use in testing the performance of species richness estimators, with a literature review of estimator performance. Ecography 28:815–829.

Whittington, J., M. Hebblewhite, and R. B. Chandler. 2018. Generalized spatial mark–resight models with an application to grizzly bears. Journal of Applied Ecology 55:157–168.

SUPPORTING INFORMATION

DATA AVAILABILITY

An associated R script is available on Zenodo: http://doi.org/10.5281/zenodo.3647866.